JACS
JOURNAL OF THE AMERICAN CHEMICAL SOCIETY
Article
pubs.acs.org/JACS

# Electrooxidation of Ethanol and Methanol Using the Molecular Catalyst $[\{Ru_4O_4(OH)_2(H_2O)_4\}(\gamma\text{-}SiW_{10}O_{36})_2]^{10-}$

YuPing Liu, Shu-Feng Zhao, Si-Xuan Guo, Alan M. Bond,* and Jie Zhang*

School of Chemistry and ARC Centre of Excellence for Electromaterials Science, Monash University, Clayton, Victoria 3800, Australia

Guibo Zhu, Craig L. Hill, and Yurii V. Geletii

Department of Chemistry, Emory University, 1515 Dickey Drive, Atlanta, Georgia 30322, United States

Supporting Information

**ABSTRACT:** Highly efficient electrocatalytic oxidation of ethanol and methanol has been achieved using the ruthenium-containing polyoxometalate molecular catalyst, $[\{Ru_4O_4(OH)_2(H_2O)_4\}(\gamma\text{-}SiW_{10}O_{36})_2]^{10-}$ ($[\mathbf{1}(\gamma\text{-}SiW_{10}O_{36})_2]^{10-}$). Voltammetric studies with dissolved and surface-confined forms of $[\mathbf{1}(\gamma\text{-}SiW_{10}O_{36})_2]^{10-}$ suggest that the oxidized forms of **1** can act as active catalysts for alcohol oxidation in both aqueous (over a wide pH range covering acidic, neutral, and alkaline) and alcohol media. Under these conditions, the initial form of **1** also exhibits considerable reactivity, especially in neutral solution containing 1.0 M $NaNO_3$. To identify the oxidation products, preparative scale bulk electrolysis experiments were undertaken. The products detected by NMR, gas chromatography (GC), and GC-mass spectrometry from oxidation of ethanol are 1,1-diethoxyethane and ethyl acetate formed from condensation of acetaldehyde or acetic acid with excess ethanol. Similarly, the oxidation of methanol generates formaldehyde and formic acid which then condense with methanol to form dimethoxymethane and methyl formate, respectively. These results demonstrate that electrocatalytic oxidation of ethanol and methanol occurs via two- and four-electron oxidation processes to yield aldehydes and acids. The total faradaic efficiencies of electrocatalytic oxidation of both alcohols exceed 94%. The numbers of aldehyde and acid products per catalyst were also calculated and compared with the literature reported values. The results suggest that **1** is one of the most active molecular electrocatalysts for methanol and ethanol oxidation.

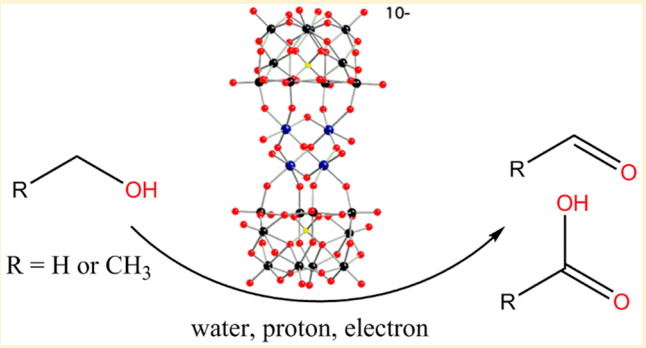


## 1. INTRODUCTION

Catalytic oxidation of an alcohol by oxygen can be used to generate electricity in electrochemical devices known as direct alcohol fuel cells (DAFCs).[1] The most widely studied ones utilize methanol and ethanol and are known as a direct methanol fuel cell (DMFC) or a direct ethanol fuel cell (DEFC), respectively. Ideally, the products of alcohol fuel cells should be $CO_2$ and $H_2O$ in order to release the maximum possible energy. Under standard conditions, oxidation of 1 mol of methanol would generate 6 mol of electrons and 1 mol of $CO_2$ with a standard reversible potential $E^0$ of 0.016 V vs SHE, as in eq 1, whereas for ethanol, 2 mol of $CO_2$ and 12 mol of electrons are generated with an $E^0$ value of 0.084 V vs SHE,[2] according to eq 2

$$CH_3OH + H_2O \rightarrow CO_2 + 6H^+ + 6e^- \quad E^0 = 0.016 \text{ V vs SHE} \qquad (1)$$

$$CH_3CH_2OH + 3H_2O \rightarrow 2CO_2 + 12H^+ + 12e^- \quad E^0 = 0.084 \text{ V vs SHE} \qquad (2)$$

Unfortunately, the electrooxidation of methanol and ethanol are kinetically slow processes with overpotentials of 0.3−0.4 V for ethanol[3] and 0.45 V for methanol[4] even using state-of-the-art catalysts. Platinum (Pt) is commonly employed as the catalyst in acidic media in DMFC or DEFC devices. However, Pt on its own is not a highly efficient catalyst due to poisoning from the strongly adsorbed species such as $CH_{(ad)}$, $CH_{3(ad)}$, and $CO_{(ad)}$ generated during oxidation.[3,5] Addition of ruthenium or tin has been reported to increase the surface coverage of oxygenated species such as $OH_{(ad)}$ and hence eliminate the adsorbed intermediates by oxidation to $CO_2$[6,7] or facilitate formate formation[8] and thus improve the catalytic activity of Pt. $OH_{(ad)}$ species generated from $H_2O_{(ad)}$ oxidation ($E^0$ = 0.49 V vs SHE) on the surface of Pt(111) is proposed to be the rate-limiting step and the origin of the overpotential for ethanol oxidation.[3] Since this step is also critical in water oxidation catalysis,[9] molecular catalysts for water oxidation also should have the ability to

Received: November 1, 2015
Published: February 5, 2016





DOI: 10.1021/jacs.5b11408
J. Am. Chem. Soc. 2016, 138, 2617−2628

catalyze alcohol oxidation. Meyer and co-workers have studied the reactivity of four well-known water oxidation intermediates $Ru^{IV}{=}O^{2+}$, $Ru^{IV}(OH)^{3+}$, $Ru^{V}{=}O^{3+}$, and $Ru^{V}(OO)^{3+}$ for benzyl alcohol oxidation. They found that $Ru^{V}(OO)^{3+}$ and $Ru^{IV}(OH)^{3+}$ are about 3 orders of magnitude more reactive compared with $Ru^{IV}{=}O^{2+}$.[10]

Polyoxometalates (POMs) are stable anion clusters that consist of multiple transition metal oxyanions linked together by shared oxygen atoms to form a large, closed 3D framework.[11] POMs exhibit a wide range of structural, redox, and catalytic properties both in the dark and under illumination with light.[11] Of particular relevance to the current study, POMs can undergo a series of reversible electron transfer processes, which are often coupled with proton transfer reactions[12,13] as needed for catalytic alcohol oxidation. In 2008, the Hill[14] and Bonchio[15] groups reported a ruthenium-containing POM, $[\{Ru_4O_4(OH)_2(H_2O)_4\}(\gamma\text{-}SiW_{10}O_{36})_2]^{10-}$ ($[\mathbf{1}(\gamma\text{-}SiW_{10}O_{36})_2]^{10-}$, structure shown in Figure 1), that exhibits excellent water oxidation

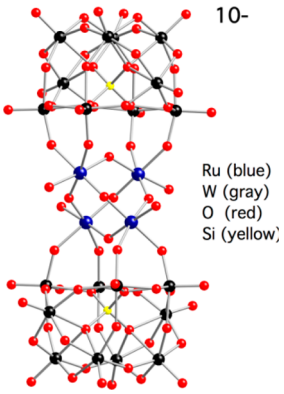


**Figure 1.** Structure of $[\mathbf{1}(\gamma\text{-}SiW_{10}O_{36})_2]^{10-}$.[17]

catalytic activity. In a subsequent catalytic study with $[\mathbf{1}(\gamma\text{-}SiW_{10}O_{36})_2]^{10-}$ linked to polyamidoamine ammonium dendrimers functionalized multiwalled carbon nanotubes, a turnover frequency (TOF) was determined to be 36 $h^{-1}$ (0.01 $s^{-1}$) at an overpotential of 0.35 V at pH 7.0.[16] Much improved catalytic activity with a TOF value of 0.82 $s^{-1}$ at an overpotential of 0.35 V at pH 7.5 has been achieved when $[\mathbf{1}(\gamma\text{-}SiW_{10}O_{36})_2]^{10-}$ was immobilized directly on reduced graphene oxide.[17]

In this study, $[\mathbf{1}(\gamma\text{-}SiW_{10}O_{36})_2]^{10-}$ was applied to electrooxidation of methanol and ethanol in both aqueous and alcohol media. The comprehensive electrochemical data available for this POM over a wide range of pH and electrolyte conditions obtained in previous studies[18,19] facilitated the investigation of the electrocatalytic properties of **1** for alcohol oxidation.

## 2. EXPERIMENTAL SECTION

**2.1. Reagents.** $Rb_8K_2$-$[\mathbf{1}(\gamma\text{-}SiW_{10}O_{36})_2]$ was synthesized as described elsewhere.[14] The chemicals ferrocene (Fc ≥98%, Sigma-Aldrich); potassium nitrate ($KNO_3$, ISO, Reag. Ph Eur grade, ≥99%, Merck); sodium nitrate ($NaNO_3$, AR grade, BDH); $Na_2HPO_4$ and $NaH_2PO_4$ (Fluka, AR grade); sulfuric acid ($H_2SO_4$, 98%, Ajax); acetic acid (AR grade, Univar); ethanol and methanol (absolute GR, 99.7%, Merck); formic acid (reagent grade, ≥95%, Sigma-Aldrich); *p*-toluenesulfonic acid monohydrate (ACS reagent, ≥98.5%, Sigma-Aldrich); 2,4-dinitrophenylhydrazine (2,4-DNPH, reagent grade, 97%, Sigma-Aldrich); formaldehyde solution (37 wt % in $H_2O$, contains 10−15% of methanol as stabilizer to prevent polymerization); acetaldehyde-2,4-DNPH (analytical standard, Sigma-Aldrich); dimethyl sulfoxide-$d_6$ (MagniSolv, deuteration degree ≥99.8%, Merck); Tetramethylsilane (TMS, MagniSolv, deuteration degree ≥99.65%, Merck); $D_2O$ (MagniSolv, deuteration degree ≥99.9%, Merck); cyclohexane (UvaSol grade, ≥99.9%, Merck); and ethyl acetate (GR, 99%, Merck) were used as supplied by the manufacturer. Poly(diallyldimethylammonium chloride) solution (PDDA, 20 wt % in water, structure shown in Figure 2) was also used as supplied by Sigma-Aldrich. Water was purified with a

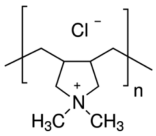


**Figure 2.** Structure of poly(diallyldimethylammonium chloride).

Milli-Q-MilliRho purification system (resistivity 18 MΩ cm) and was used to prepare all aqueous electrolyte solutions. To acidify alcohol solutions, concentrated $H_2SO_4$ (98%) was slowly added to ethanol or methanol until a concentration of 0.50 M $H_2SO_4$ was achieved. Sodium phosphate buffer (PB) solutions of 0.10 or 0.40 M were prepared by mixing 0.10 M $Na_2HPO_4$ and 0.10 M $NaH_2PO_4$ solutions or 0.40 M $Na_2HPO_4$ and 0.40 M $NaH_2PO_4$ solutions to achieve pH 7.0. Carbon cloth (thickness of 2 mm, Tsukuba Materials Information Laboratory) was cut into 2.0 cm × 2.0 cm square pieces. They were washed with water and acetone and then dried before use as electrodes.

**2.2. Fabrication of $[\mathbf{1}(\gamma\text{-}SiW_{10}O_{36})_2]^{10-}$/PDDA-Modified Electrodes.** Under vigorous stirring, 5 μL of 20% (wt % in water) PDDA was added to 5 mL of aqueous solution containing 0.20 mM $[\mathbf{1}(\gamma\text{-}SiW_{10}O_{36})_2]^{10-}$ to form a water-insoluble composite. After centrifuging at 4000 rpm for 3 min and discarding the supernatant, the resultant precipitate was collected and washed twice with water. Finally, the solid was redispersed in 1 mL of water. To modify the carbon cloth electrodes, 200 μL of the dispersion was drop cast on the electrode surface (2.0 cm × 2.0 cm). For the modification of glassy carbon electrodes (3.0 mm diameter), this dispersion was first diluted 5 times with water, and 3 μL of the diluted dispersion was used for drop casting. To estimate the surface concentration (Γ) of electrochemically active $[\mathbf{1}(\gamma\text{-}SiW_{10}O_{36})_2]^{10-}$, background subtracted linear sweep dc voltammetric responses associated with the first one-electron oxidation or reduction processes of the Ru centers were integrated to obtain the charge consumed, which is related to the amount of electrochemically active $[\mathbf{1}(\gamma\text{-}SiW_{10}O_{36})_2]^{10-}$ by Faraday's law.[13]

**2.3. Electrochemical Measurements.** Conventional dc cyclic, linear sweep, and rotating disk electrode (RDE) voltammetric experiments were carried out using a CHI 700D electrochemical workstation (CH Instruments, Austin, Texas, USA). A rotating disk electrode rotator (RRDE-3A, ALS, Japan) connected to the workstation was employed in the RDE experiments. Fourier transformed large amplitude ac (FTAC) voltammetric measurements were undertaken with a home-built apparatus,[20] using an applied sine wave perturbation (amplitude 80 mV and frequency 9.02 Hz) superimposed onto the dc ramp. The total current measured was then subjected to Fourier transformation to obtain the power spectrum. After selection of the frequency band of interest, inverse Fourier transformation was used to generate the required aperiodic dc and ac harmonic components.[20−22]

All voltammograms were acquired at 22 ± 2 °C using a standard three-electrode electrochemical cell arrangement with a glassy carbon working electrode (1.0 mm diameter, from ALS, Japan, or 3.0 mm diameter, CH Instruments, Austin, Texas, USA) and a Pt wire counter electrode. In alcohol media, a Pt wire quasi-reference electrode contained in a glass tube with a vycor frit filled with alcohol (0.50 M $H_2SO_4$) solution was used and its potential calibrated against that of the ferrocene/ferricenium ($Fc/Fc^+$) couple. In aqueous media, a $Hg/HgSO_4$ (saturated $K_2SO_4$ solution) reference electrode was used. Thus, the potential values obtained in alcohol media are reported against the $Fc/Fc^+$ reference process, while those obtained in aqueous media are reported against the $Hg/HgSO_4$ reference process, which is 0.64 V vs NHE.[23] A glassy carbon working electrode (3.0 mm diameter) was used for the RDE voltammetric studies along with the same reference and counter electrodes employed in dc and FTAC voltammetry. Prior to


DOI: 10.1021/jacs.5b11408
J. Am. Chem. Soc. 2016, 138, 2617−2628

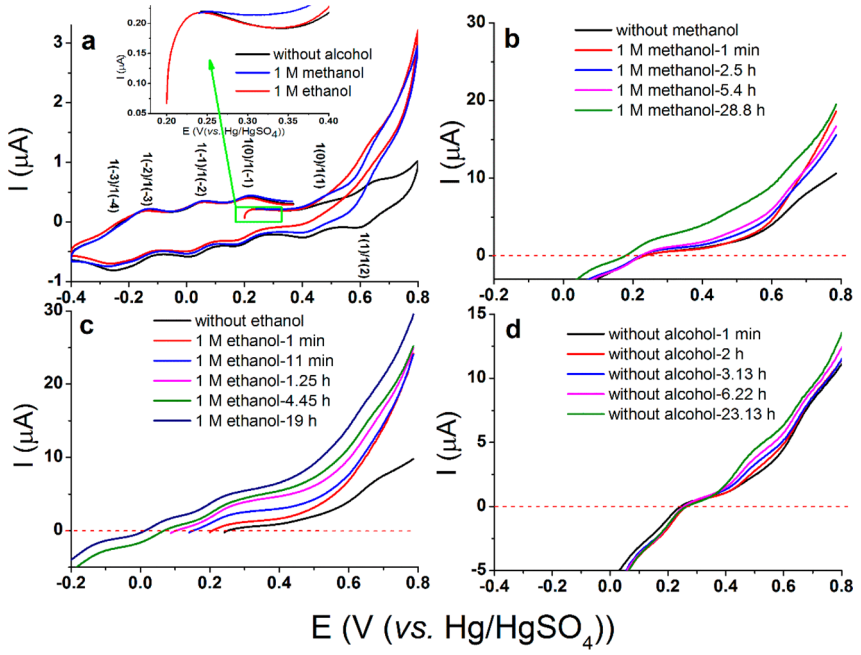


**Figure 3.** (a) Cyclic voltammograms of 0.50 mM $[\mathbf{1}(\gamma\text{-SiW}_{10}\text{O}_{36})_2]^{10-}$ in aqueous 2.0 M $H_2SO_4$ without alcohol (black line) and with 1.0 M ethanol (red line) or methanol (blue line), obtained at a 1.0 mm diameter glassy carbon electrode with a scan rate of 0.05 V $s^{-1}$. The inset figure shows a zoom-in of the region close to the initial potential. (b) RDE voltammograms of 0.30 mM $[\mathbf{1}(\gamma\text{-SiW}_{10}\text{O}_{36})_2]^{10-}$ in aqueous 2.0 M $H_2SO_4$ obtained at a 3.0 mm diameter glassy carbon RDE with a scan rate of 0.02 V $s^{-1}$, before and after the addition of 1.0 M methanol for the indicated periods of time. (c) As for (b), but with 1.0 M ethanol. (d) As for (b), but without alcohol, in order to provide a comparison with (b) and (c).

each voltammetric experiment, the working electrode was polished using an aqueous 0.3 $\mu$m alumina slurry on a polishing cloth (Buehler), rinsed with water, and then sonicated to remove residual alumina, before a final rinse with water. The initial potential for the transient cyclic voltammetric measurements unless otherwise stated was chosen to be the open-circuit potential. Bulk electrolysis was carried out with a carbon cloth (2 mm × 2.0 cm × 2.0 cm) working electrode and a large area Pt mesh counter electrode in a two-compartment cell, along with the same reference electrode used in voltammetric studies.

**2.4. Product Analysis.** NMR experiments were undertaken with a Bruker DRX400 spectrometer at frequencies of 400.2 MHz ($^1$H spectra) and 100.63 MHz ($^{13}$C spectra). For qualitative studies, 0.14 mL of dimethyl sulfoxide-$d_6$ was added into 0.7 mL of ethanol or methanol solution. For quantitative ones, 0.14 mL of dimethyl sulfoxide-$d_6$ along with 10 mM of the internal standard cyclohexane was used in alcohol media, while 0.14 mL of $D_2O$ with 50 mM *p*-toluenesulfonic acid solution was added into the aqueous solutions after bulk electrolysis. The relaxation delay was confirmed to be long enough to ensure the validity of comparing integrated resonances. The $^1$H and $^{13}$C resonances of dimethyl sulfoxide-$d_6$ were calibrated as 2.5 and 39.5 ppm vs TMS, respectively.

Gas chromatography (GC) was performed with an Agilent 7820A system equipped with an Agilent HP-5 column with dimensions of 30 m × 0.32 $\mu$m and a film thickness of 0.25 $\mu$m or a SGE 25QC3/BP20 WAX column with dimensions of 25 m × 0.32 $\mu$m and a film thickness of 1.0 $\mu$m. The retention times were compared with those of authentic compounds. GC-MS analysis was undertaken using an HP 6890A gas chromatograph equipped with an Agilent 5973 N mass selective detector.

High-performance liquid chromatography (HPLC) was undertaken with an Agilent 1220 Infinity LC system equipped with a C18 column (AlltechAlltima, Waters standard, particle size of 5 $\mu$m, dimensions of 4.6 mm × 150 mm, Grace Davison Discovery Science) and UV−visible spectroscopic detection at a wavelength of 365 nm. Solution A of the mobile phase was acetonitrile, and solution B was 10/90 v/v methanol/$H_2O$. HPLC was carried out with a linear gradient from 20% A to 100% A for 10 min and then held for 2 min followed by a linear gradient from 100% A to 20% A and 80% B for 5 min. The flow rate of the mobile phase was 0.8 mL $min^{-1}$. Acetaldehyde was derivatized with 2,4-DNPH in a 50/50 v/v $H_2O$/acetonitrile solution containing 0.20 M $H_2SO_4$ and 2,4-DNPH in excess. The retention times were compared with those of authentic compounds.

## 3. RESULTS AND DISCUSSION

**3.1. Electrocatalytic Oxidation of Alcohols by 1 in Aqueous Media.** *3.1.1. Electrochemistry of $[\mathbf{1}(\gamma\text{-SiW}_{10}\text{O}_{36})_2]^{10-}$ Dissolved in Acidic and Neutral Solutions.* Cyclic voltammetric studies were undertaken in 2.0 M aqueous $H_2SO_4$ solution containing 0.50 mM $[\mathbf{1}(\gamma\text{-SiW}_{10}\text{O}_{36})_2]^{10-}$. In this highly acidic medium, six processes associated with the $Ru^{IV}$ centers were observed (Figure 3(a), black trace). Following the nomenclature adopted in our previous studies,[17−19] processes $\mathbf{1}(0)/\mathbf{1}(1)$ and $\mathbf{1}(1)/\mathbf{1}(2)$ are assigned to the one-electron oxidation of the $Ru^{IV}$ centers and processes $\mathbf{1}(0)/\mathbf{1}(-1)$, $\mathbf{1}(-1)/\mathbf{1}(-2)$, $\mathbf{1}(-2)/\mathbf{1}(-3)$, and $\mathbf{1}(-3)/\mathbf{1}(-4)$ to the sequential one-electron reduction of the $Ru^{IV}$ centers. The first $\mathbf{1}(0)/\mathbf{1}(1)$ oxidation process is less well-defined than process $\mathbf{1}(1)/\mathbf{1}(2)$. Reduction processes $\mathbf{1}(-2)/\mathbf{1}(-3)$ and $\mathbf{1}(-3)/\mathbf{1}(-4)$ are less well-resolved than the $\mathbf{1}(0)/\mathbf{1}(-1)$ and $\mathbf{1}(-1)/\mathbf{1}(-2)$ ones and almost merge into a two-electron process. These results are consistent with those reported previously in aqueous $H_2SO_4$.[17,18] Processes derived from the reduction of the $W^{VI}$ centers at more negative potential region and those that led to the formation of highly active water oxidation catalysts at more positive potential region[18] are not considered in this study which focuses on the oxidation of alcohol using the catalytically active $Ru^{IV}$ centers.

Reversible potentials ($E^{0\prime}$) and peak-to-peak separations ($\Delta E_p$) for each process were derived from cyclic voltammograms of $[\mathbf{1}(\gamma\text{-SiW}_{10}\text{O}_{36})_2]^{10-}$ obtained in 2.0 M $H_2SO_4$. Assuming the diffusion coefficients of both reduced and oxidized forms are equal, $E^{0\prime}$ can be calculated from the midpoint potential which is the average of the reduction ($E_p^{red}$) and oxidation ($E_p^{ox}$) peak potentials ($E^{0\prime} = (E_p^{ox} + E_p^{red})/2$). $\Delta E_p = E_p^{ox} - E_p^{red}$ values for all six


DOI: 10.1021/jacs.5b11408
J. Am. Chem. Soc. 2016, 138, 2617−2628

ruthenium-based one-electron processes are close to the theoretical value of 56 mV predicted for a reversible one-electron transfer process at 22 °C.[23] $E^{0\prime}$ values for reduction processes $\mathbf{1}(0)/\mathbf{1}(-1)$, $\mathbf{1}(-1)/\mathbf{1}(-2)$, $\mathbf{1}(-2)/\mathbf{1}(-3)$, and $\mathbf{1}(-3)/\mathbf{1}(-4)$ are 0.198, 0.039, −0.161, and −0.241 V, respectively, and those for the oxidation processes $\mathbf{1}(0)/\mathbf{1}(1)$ and $\mathbf{1}(1)/\mathbf{1}(2)$ are 0.435 and 0.625 V, respectively.

Upon addition of 1.0 M ethanol or methanol (Figure 3(a), red and blue traces, respectively), a small decrease in background current and peak current is evident for the reduction processes. By contrast, current increases are seen for both oxidation processes ($\mathbf{1}(0)/\mathbf{1}(1)$ and $\mathbf{1}(1)/\mathbf{1}(2)$) upon the addition of alcohol, which are assigned to the catalytic oxidation of alcohol. Moreover, $\mathbf{1}(2)$ shows higher catalytic activity than $\mathbf{1}(1)$ as evidenced by the larger increase in current magnitude. The simplified mechanisms for the $\mathbf{1}(0)/\mathbf{1}(1)$ and $\mathbf{1}(1)/\mathbf{1}(2)$ catalyzed ethanol oxidation reactions are illustrated by Schemes 1(a) and 1(b), respectively. It is assumed that the catalytic

**Scheme 1. Reaction Pathways Proposed for $[\mathbf{1}(\gamma\text{-}SiW_{10}O_{36})_2]^{10-}$-Catalyzed Eletrooxidation of Ethanol in an Acidic Medium**

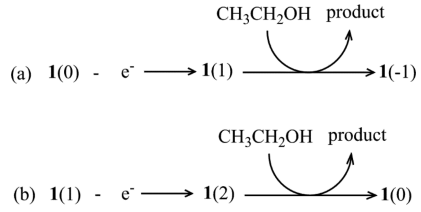


oxidation processes involve an overall two-electron transfer reaction in each step, which is commonly observed in irreversible oxidation of organic compounds.[24] Analogous reaction schemes are applicable to the electrocatalytic oxidation of methanol. The onset potential for detection of catalytic current was approximately 0.4 V for both alcohols in the acidic aqueous medium.

Careful inspection of the voltammetric data reveals that addition of 1.0 M alcohol, ethanol in particular, generated a small negative shift in the open-circuit potential (Figure 3(a)). This observation suggests that $\mathbf{1}(0)$ is spontaneously reduced by the alcohols. To confirm this hypothesis, RDE experiments were undertaken after addition of alcohol to monitor the change in the voltammetric response associated with $\mathbf{1}(0)$ over a period of about 20 h. The RDE results clearly show a shift in the potential where current is zero (approximately corresponds to the open-circuit potential) toward more negative values and a shift of the plateau current in the positive current direction (Figures 3(b) and 3(c)), especially in the case of ethanol (Figure 3(c)). In particular, the RDE voltammograms obtained after about 1 day indicate the formation of a high concentration of reduced $\mathbf{1}(-1)$ and $\mathbf{1}(-2)$ in the methanol and ethanol solutions, respectively, as judged by the shift in zero current potential with respect to the reversible potentials associated with **1**. By contrast, no shift in either the zero current potential or the plateau current was observed in the absence of alcohol (Figure 3(d)). However, the observed shift in the half wave potential associated with the first oxidation process also implies that a change occurs in the electrode kinetics.[25] This hypothesis is supported by the cyclic voltammetric data which indicate a decrease in peak-to-peak separation over time (Figure S1). Since the highly negatively charged $\mathbf{1}(0)$ forms strong ion pairs with cations in the electrolyte media,[19] in the presence of 2.0 M $H_2SO_4$, an exchange between the proton and the original counter cations (i.e., $Rb^+$ and/or $K^+$) is expected and presumably generates a kinetically more facile form of $\mathbf{1}(0)$.

On the basis of the above observations and keeping in mind the fact that the overall irreversible electron transfer reactions in organic chemistry normally involve even numbers of electrons,[24] it is assumed that $\mathbf{1}(0)$ is initially reduced by ethanol to the $\mathbf{1}(-2)$ state, which is then quickly oxidized by $\mathbf{1}(0)$ to form 2 equiv of $\mathbf{1}(-1)$, as shown in Scheme 2. The reaction product, $\mathbf{1}(-1)$, also

**Scheme 2. Proposed Mechanism for the Spontaneous Reduction of 1(0) by Ethanol**

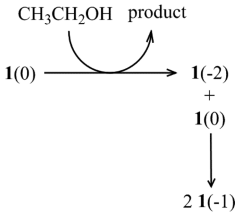


oxidizes alcohols but at a significantly slower rate than $\mathbf{1}(0)$. By contrast, the analogous reduction reactions with methanol are much slower (Figure 3(b)), even though they are slightly more favorable in a thermodynamic sense.[3,26,27]

To establish the impact of pH and the supporting electrolyte, cyclic voltammetry and catalytic activity of 0.50 mM $[\mathbf{1}(\gamma\text{-}SiW_{10}O_{36})_2]^{10-}$ were also studied in 0.10 M PB solution at pH 7.0 with either 1.0 M $NaNO_3$ or 1.0 M $KNO_3$ as an additional supporting electrolyte (Figure 4, black trace). Since $[\mathbf{1}(\gamma\text{-}SiW_{10}O_{36})_2]^{10-}$ is very negatively charged, high concentrations of supporting electrolyte were introduced to minimize the electrostatic effect so that well-defined voltammograms were obtained.[19] Under these conditions, processes $\mathbf{1}(-2)/\mathbf{1}(-3)$ and $\mathbf{1}(-3)/\mathbf{1}(-4)$ merged to give a two-electron reduction process $\mathbf{1}(-2)/\mathbf{1}(-4)$ with $E^{0\prime}$ and $\Delta E_p$ values of ~ −0.62 V and 92 mV, respectively, in the presence of either 1.0 M $NaNO_3$ or 1.0 M

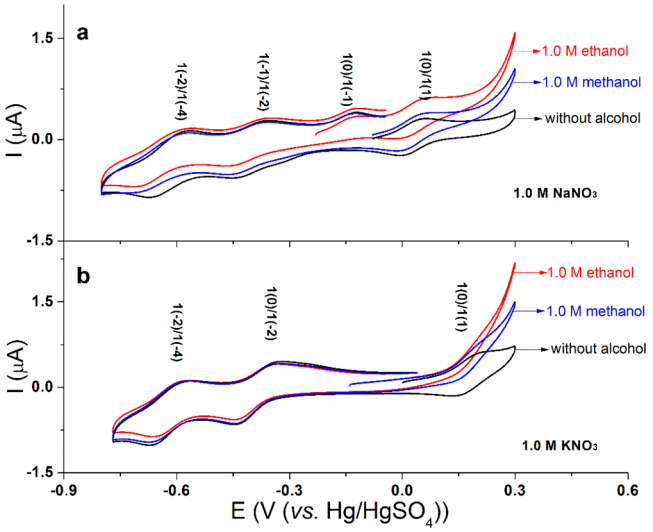


**Figure 4.** (a) Cyclic voltammograms of 0.50 mM $[\mathbf{1}(\gamma\text{-}SiW_{10}O_{36})_2]^{10-}$ in 0.10 M PB solution (pH 7.0) containing 1.0 M $NaNO_3$ without alcohol (black line) and with 1.0 M ethanol (red line) or methanol (blue line), obtained at a 1.0 mm diameter glassy carbon electrode with a scan rate of 0.05 V $s^{-1}$. (b) As for (a), but with 1.0 M $KNO_3$ as the additional supporting electrolyte.



DOI: 10.1021/jacs.5b11408
J. Am. Chem. Soc. 2016, 138, 2617−2628

$KNO_3$. Processes $\mathbf{1}(0)/\mathbf{1}(-1)$ and $\mathbf{1}(-1)/\mathbf{1}(-2)$ remain resolved with $E^{0\prime}$ and $\Delta E_p$ values of −0.216 V and 185 mV for $\mathbf{1}(0)/\mathbf{1}(-1)$ and −0.399 V and 84 mV for $\mathbf{1}(-1)/\mathbf{1}(-2)$, respectively, in the presence of 1.0 M $NaNO_3$. With 1.0 M $KNO_3$ as the additional supporting electrolyte, these processes merge into a two-electron reduction process $\mathbf{1}(0)/\mathbf{1}(-2)$ with $E^{0\prime}$ and $\Delta E_p$ values of −0.386 V and 113 mV, respectively. The one-electron $\mathbf{1}(0)/\mathbf{1}(1)$ oxidation process has a more negative $E^{0\prime}$ value of 0.026 V with $NaNO_3$ present than that of 0.173 V with $KNO_3$ as the additional electrolyte, as noted previously,[19] while $\Delta E_p$ values are about 61 mV in both cases. As reported previously, the two one-electron $\mathbf{1}(1)/\mathbf{1}(2)$ and $\mathbf{1}(2)/\mathbf{1}(3)$ oxidation processes merge into a one-step two-electron oxidation process and exhibit some water oxidation catalytic activity at pH 7.0.[19]

Upon addition of 1.0 M ethanol or 1.0 M methanol in the pH 7.0 buffer solutions (Figure 4, red and blue traces), the reduction processes exhibit a small decrease in background and peak currents, as also found in 2.0 M $H_2SO_4$. Again, significant current enhancement is observed for the $\mathbf{1}(0)/\mathbf{1}(1)$ oxidation process upon the addition of alcohols. With $NaNO_3$ as the additional supporting electrolyte, upon addition of 1.0 M ethanol, the open-circuit potential shifted to a more negative value (Figure 4(a)), indicating that $\mathbf{1}(0)$ has been reduced spontaneously by ethanol to the $\mathbf{1}(-1)$ state. This has been confirmed by RDE measurements (Figures S2(b) and (c)). The RDE voltammograms (Figure S2(c)) show that $\mathbf{1}(0)$ is reduced to $\mathbf{1}(-1)$ in less than 1 min in the presence of 1.0 M ethanol. Then, $\mathbf{1}(-1)$ is further reduced to $\mathbf{1}(-2)$. A significant amount of $\mathbf{1}(-2)$ was formed after 1 h. By contrast, reduction of $\mathbf{1}(0)$ by methanol is much slower. The complete reduction of $\mathbf{1}(0)$ to $\mathbf{1}(-1)$ by methanol takes about 0.5 h (Figure S2(b)). Again, $\mathbf{1}(-1)$ was then very slowly further reduced to $\mathbf{1}(-2)$. After 20 h, only a small amount of $\mathbf{1}(-2)$ was produced. Again, as found in the aqueous 2.0 M $H_2SO_4$ medium, no negative shift in the zero current potential occurred in the absence of alcohol (Figure S2(d)). Thus, Scheme 2 and its analogous forms are also assumed to be applicable under these conditions. With $KNO_3$ as the additional supporting electrolyte, a significant negative shift of open-circuit potential also was observed upon addition of either methanol or ethanol (Figure 4(b)). However, reduction of $\mathbf{1}(0)$ was much slower, as suggested by the RDE experiments (Figure S3). This observation is consistent with the less favorable reaction thermodynamics determined by comparison of the reversible potentials of process $\mathbf{1}(0)/\mathbf{1}(-1)$ in Figure 4(a) and process $\mathbf{1}(0)/\mathbf{1}(-2)$ in Figure 4(b).

*3.1.2. Voltammetry of Surface-Confined [1(γ-$SiW_{10}O_{36})_2]^{10-}$.* The voltammograms obtained with a $[\mathbf{1}(\gamma\text{-}SiW_{10}O_{36})_2]^{10-}$/PDDA-modified glassy carbon electrode are shown in Figure 5. Two reduction processes are observed, with $E^{0\prime}$ values of 0.198 V ($\Delta E_p$ = 37 mV) and 0.035 V ($\Delta E_p$ = 53 mV). These processes resemble the reduction processes $\mathbf{1}(0)/\mathbf{1}(-1)$ and $\mathbf{1}(-1)/\mathbf{1}(-2)$ in solution. However, the peak current (area) for the process at 0.035 V is significantly larger than that for the process at 0.198 V, which indicates that the second reduction process may involve more than one electron. No further reduction was detected when the potential was scanned to as negative as −0.4 V. A well-defined oxidation process observed at 0.623 V ($\Delta E_p$ = 44 mV) is attributed to the one-electron oxidation of $\mathbf{1}(0)$ since its peak height is comparable to that associated with the $\mathbf{1}(0)/\mathbf{1}(-1)$ process. Since the half-wave potentials associated with the electrocatalytic processes are similar to the reversible potential of this oxidation process, the

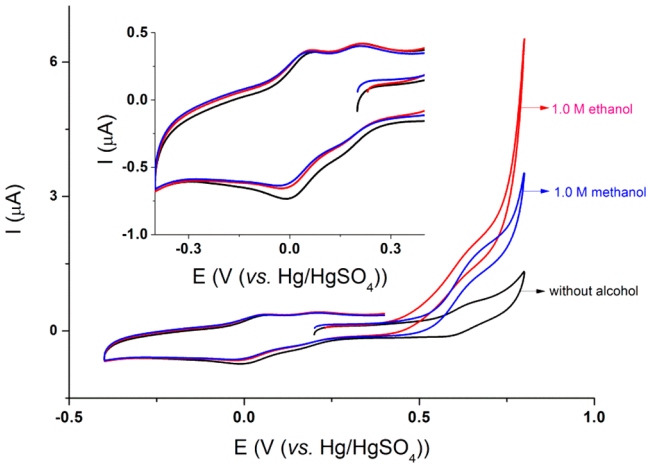


**Figure 5.** Cyclic voltammograms obtained at a 3.0 mm diameter glassy carbon electrode modified with 3 μL of $[\mathbf{1}(\gamma\text{-}SiW_{10}O_{36})_2]^{10-}$/PDDA (Γ = 0.08 nmol/cm$^2$) with a scan rate of 0.01 V s$^{-1}$ in aqueous 2.0 M $H_2SO_4$ solution without alcohol (black line) and with 1.0 M ethanol (red line) or methanol (blue line).

oxidized form $\mathbf{1}(1)$ is considered to be the active catalyst for alcohol oxidation with surface-confined $[\mathbf{1}(\gamma\text{-}SiW_{10}O_{36})_2]^{10-}$.

In a previous study, we have shown that the electrolyte cation has a significant influence on the voltammetry of $[\mathbf{1}(\gamma\text{-}SiW_{10}O_{36})_2]^{10-}$, especially in neutral and alkaline media.[19] Therefore, the voltammetry and catalytic activity of surface-confined $[\mathbf{1}(\gamma\text{-}SiW_{10}O_{36})_2]^{10-}$ were studied in both neutral and alkaline media in the presence of 1.0 M $NaNO_3$ or $KNO_3$. In the absence of ethanol, the voltammograms obtained at pH 7.0 in the presence of 1.0 M $NaNO_3$ exhibit three reversible processes with $E^{0\prime}$ and $\Delta E_p$ values of −0.366 V and 35 mV, −0.176 V and 68 mV, and 0.003 V and 39 mV, respectively, at a scan rate of 0.01 V s$^{-1}$ (Figure 6(a)). In the presence of 1.0 M $KNO_3$, only two reversible processes are evident in the same potential region, with $E^{0\prime}$ and $\Delta E_p$ values of −0.369 V and 72 mV and 0.131 V and 54 mV, respectively (Figure 6(b)). The $E^{0\prime}$ values for these two processes are similar to those of $\mathbf{1}(0)/\mathbf{1}(-1)$ reduction and $\mathbf{1}(0)/\mathbf{1}(1)$ oxidation processes associated with the dissolved form at the same pH.[19] In aqueous 0.010 M NaOH solution with 1.0 M $NaNO_3$ as the additional supporting electrolyte, the cyclic voltammogram shows two reversible processes in the potential range of −0.6 to −0.1 V, with $E^{0\prime}$ and $\Delta E_p$ values of −0.461 V and 21 mV and −0.233 V and 40 mV, respectively (Figure 6(c)). By contrast, with 1.0 M $KNO_3$ as the additional electrolyte, only one reversible process was observed in this potential region, with $E^{0\prime}$ and $\Delta E_p$ values of −0.212 V and 29 mV, respectively (Figure 6(d)). In both cases, the processes with an $E^{0\prime}$ value of ∼ −0.2 V are assigned to the $\mathbf{1}(0)/\mathbf{1}(1)$ oxidation process, judging based on the high reactivity of the oxidized form as indicated from the large catalytic currents associated with these processes in the presence of 1.0 M ethanol. Relative to their solution-phase data,[19] these oxidation processes shifted by about 10 mV negatively in the presence of 1.0 M $KNO_3$ and 100 mV positively in the presence of 1.0 M $NaNO_3$.

In the presence of 1.0 M ethanol (Figure 6), catalytic currents were observed in all media. At pH 7.0, the onset potential with $Na^+$ is −0.26 V, which is 0.18 V less positive than that with $K^+$ at the same pH (Figures 6(a) and (b)). This implies that at pH 7.0, in the presence of $NaNO_3$, $\mathbf{1}(0)$ is able to oxidize ethanol with an appreciable rate, while under other conditions, $\mathbf{1}(1)$ is the reactive species. By contrast, the onset potentials for ethanol


DOI: 10.1021/jacs.5b11408
J. Am. Chem. Soc. 2016, 138, 2617−2628

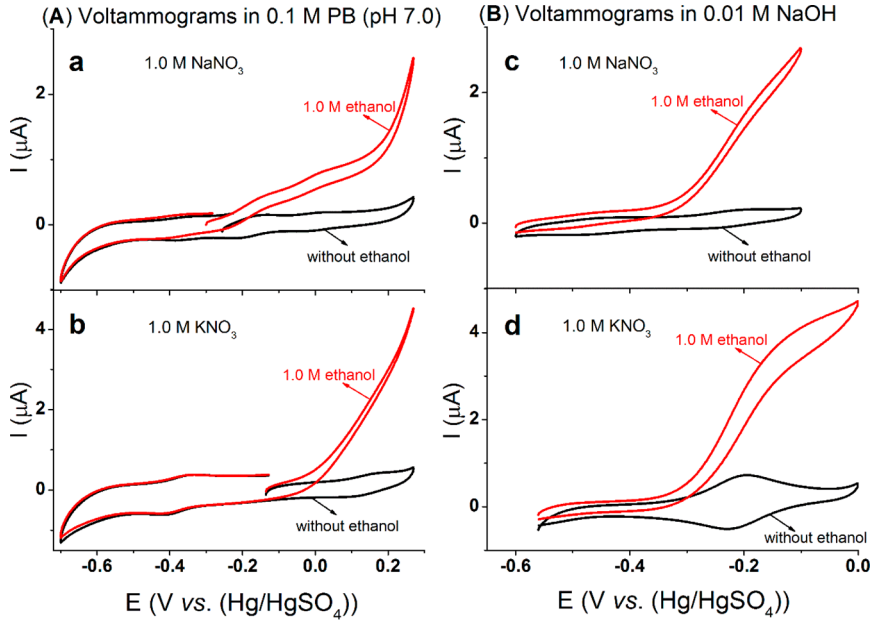


**Figure 6.** Cyclic voltammograms obtained at a 3.0 mm diameter glassy carbon electrode modified with 3 $\mu$L of $[\mathbf{1}(\gamma\text{-}SiW_{10}O_{36})_2]^{10-}$/PDDA (scan rate = 0.01 V $s^{-1}$) in the absence (black line) and presence (red line) of 1.0 M ethanol in (a) 0.10 M PB solution (pH 7.0) with 1.0 M $NaNO_3$; (b) 0.10 M PB solution (pH 7.0) with 1.0 M $KNO_3$; (c) 0.010 M NaOH solution with 1.0 M $NaNO_3$; (d) 0.010 M NaOH solution with 1.0 M $KNO_3$. $\Gamma$ = 0.02 (a), 0.04 (b), 0.05 (c), and 0.9 (d) nmol/$cm^2$.

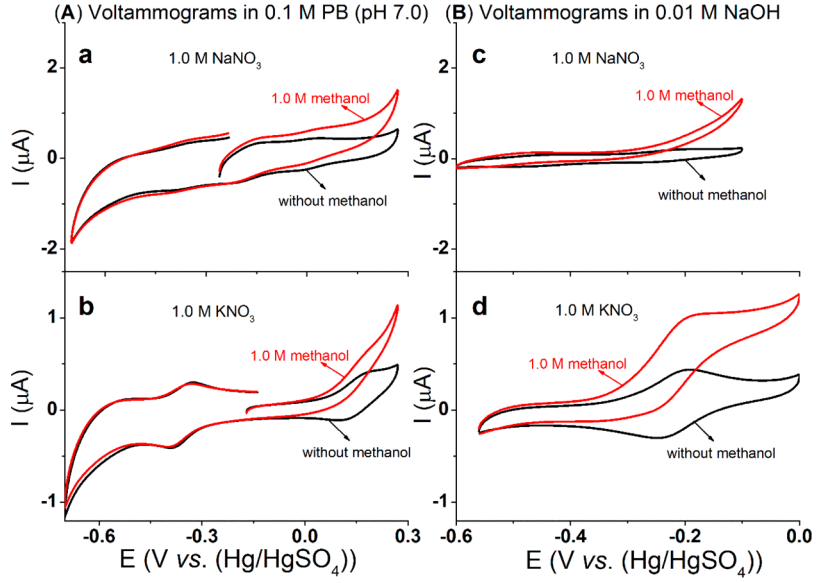


**Figure 7.** Cyclic voltammograms obtained at a 3.0 mm diameter glassy carbon electrode modified with 3 $\mu$L of $[\mathbf{1}(\gamma\text{-}SiW_{10}O_{36})_2]^{10-}$/PDDA (scan rate = 0.01 V $s^{-1}$) in the absence (black line) and in the presence (red line) of 1.0 M methanol in (a) 0.10 M PB solution (pH 7.0) with 1.0 M $NaNO_3$; (b) 0.10 M PB solution (pH 7.0) with 1.0 M $KNO_3$; (c) 0.010 M NaOH solution with 1.0 M $NaNO_3$; (d) 0.010 M NaOH solution with 1.0 M $KNO_3$. $\Gamma$ = 0.06 (a), 0.09 (b), 0.05 (c), and 0.4 (d) nmol/$cm^2$.

oxidation are ~−0.30 V in aqueous 0.010 M NaOH solutions in the presence of either 1.0 M $NaNO_3$ or 1.0 M $KNO_3$. The catalytic activity of **1**(1) is considerably higher with $NaNO_3$ as the additional electrolyte than with $KNO_3$.

Methanol oxidation in both neutral (pH 7.0) and alkaline (0.010 M NaOH) media in the presence of 1.0 M $KNO_3$ or $NaNO_3$ (Figure 7) shows the same trends, but methanol is less reactive compared to ethanol. Recently, Waymouth and co-workers reported electrocatalytic methanol oxidation in a buffered pH 11.5 aqueous solution (with 1.23 M methanol) using [($\eta^6$-*p*-cymene)($\eta^2$-*N,O*-(1*R*,2*S*)-*cis*-1-amino-2-indanol)]-$Ru^{II}Cl$ absorbed on an edge-plane graphite electrode with an onset potential of 0.56 V vs NHE (−0.08 V vs $Hg/HgSO_4$),[28] which is similar to values reported with other Ni, Ru, and Rh molecular catalysts. However, this value is ~0.290 V more positive than ours obtained under similar conditions in aqueous media containing 0.010 M NaOH and 1.0 M $KNO_3$ and is 170 mV more positive than that found in this study under neutral pH conditions where methanol oxidation is thermodynamically less favorable.

### 3.2. Electrocatalytic Oxidation of Alcohols by $[1(\gamma\text{-}SiW_{10}O_{36})_2]^{10-}$ in Acidified Alcohol Solutions.

*3.2.1. Vol-*



DOI: 10.1021/jacs.5b11408
*J. Am. Chem. Soc.* 2016, 138, 2617−2628

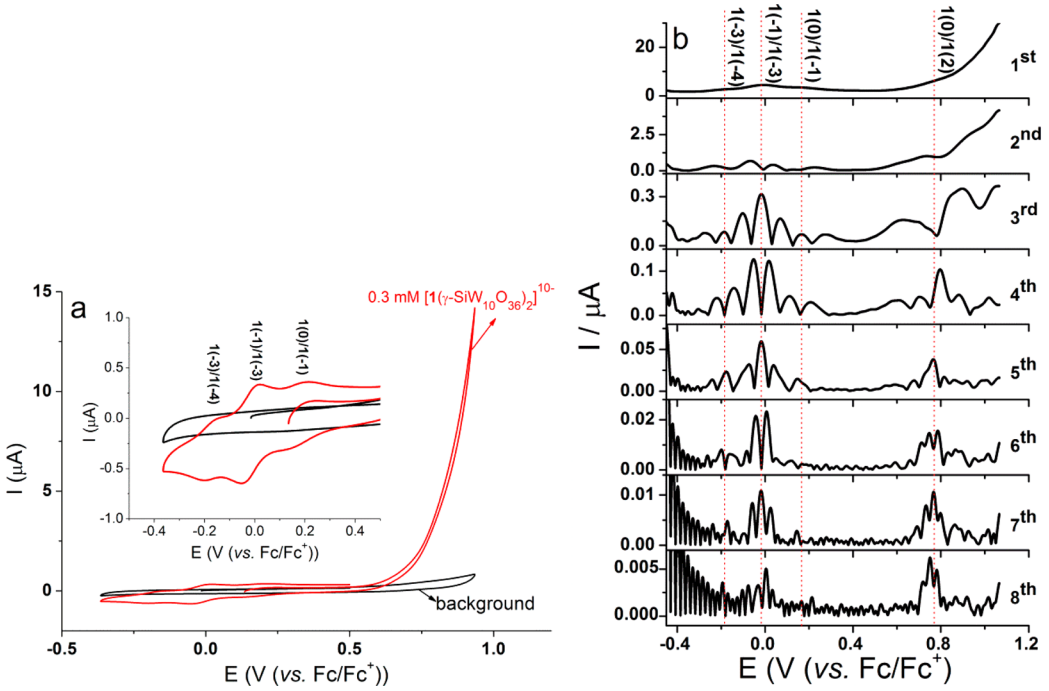


**Figure 8.** (a) Dc cyclic voltammograms (scan rate = 0.05 V $s^{-1}$) and (b) 1st to 8th harmonic components of a FTAC voltammogram ($f$ = 9.02 Hz, $\Delta E$ = 80 mV, scan rate = 126.6 mV $s^{-1}$) of 0.30 mM $[\mathbf{1}(\gamma\text{-}SiW_{10}O_{36})_2]^{10-}$ obtained at a 1.0 mm diameter glassy carbon electrode in ethanol containing 0.50 M $H_2SO_4$.

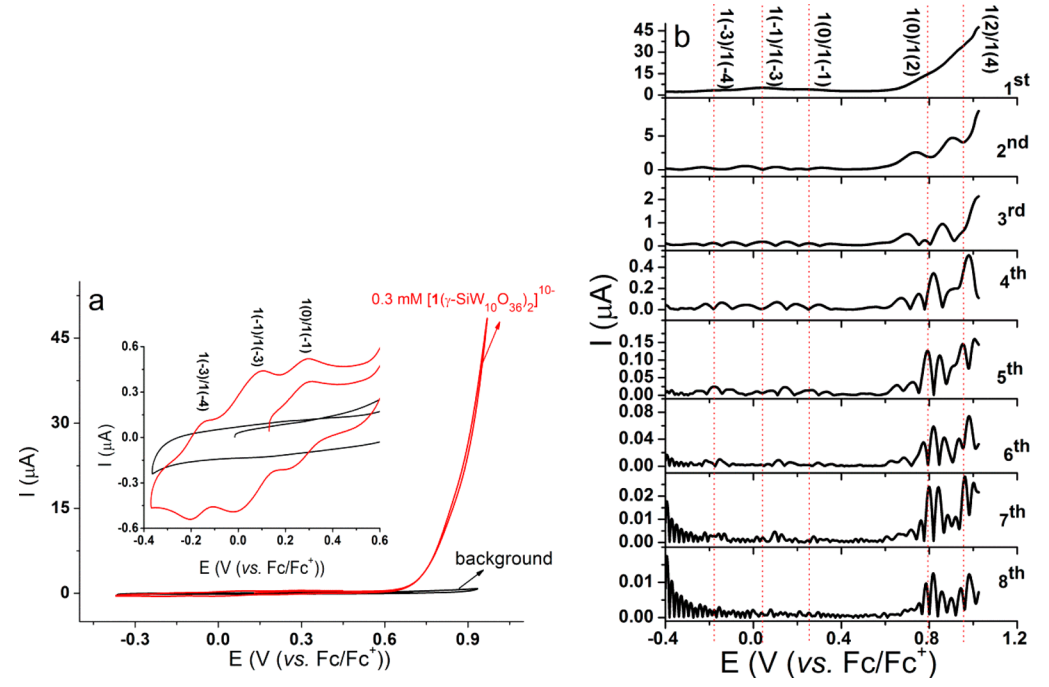


**Figure 9.** (a) Dc cyclic voltammograms (scan rate = 0.05 V $s^{-1}$) and (b) 1st to 8th harmonic components of a FTAC voltammogram ($f$ = 9.02 Hz, $\Delta E$ = 80 mV, scan rate = 108.3 mV $s^{-1}$) of 0.30 mM $[\mathbf{1}(\gamma\text{-}SiW_{10}O_{36})_2]^{10-}$ obtained at a 1.0 mm diameter glassy carbon electrode in methanol containing 0.50 M $H_2SO_4$.

*tammetry of Dissolved $[\mathbf{1}(\gamma\text{-}SiW_{10}O_{36})_2]^{10-}$.* The voltammetry of $[\mathbf{1}(\gamma\text{-}SiW_{10}O_{36})_2]^{10-}$ also was studied in acidified (0.50 M $H_2SO_4$) ethanol and methanol, under both dissolved and surface-confined formats. Under conditions relevant to Figure 8(a), the dc cyclic voltammogram of 0.30 mM $[\mathbf{1}(\gamma\text{-}SiW_{10}O_{36})_2]^{10-}$ over the potential range of 0.94 to −0.37 V in ethanol exhibits three well-defined reversible processes with $E^{0\prime}$ values of 0.178, −0.017, and −0.178 V, prior to the onset of a sharp increase in oxidation current at about 0.6 V. To estimate the reversible potential of the catalyst under turnover conditions, FTAC voltammetry was used, taking advantage of the fact that higher harmonic components in this technique are insensitive to the catalytic process.[29] Exploitation of this capability of FTAC voltammetry is crucial in this case since alcohol is both the


DOI: 10.1021/jacs.5b11408
J. Am. Chem. Soc. 2016, 138, 2617−2628

solvent and substrate for **1**, meaning that the electron transfer properties of **1** cannot be obtained in the absence of alcohol. The ac harmonics (Figure 8(b)) also display three processes at similar potentials as in dc cyclic voltammetry with that at −0.017 V having the highest current. The processes at 0.178 and −0.178 V are assigned as one-electron transfer reactions, while that at −0.017 V is an overall two-electron reduction process involving two $Ru^{IV}$ centers. Hence, these processes are assigned as **1**(0)/**1**(−1), **1**(−1)/**1**(−3), and **1**(−3)/**1**(−4), respectively (see Figure 8).[19] The fact that the open-circuit potential is more negative than the reversible potential of the **1**(0)/**1**(−1) process suggests that the initial form of **1** in these experiments is **1**(−1), due to the reduction of **1**(0) by ethanol to **1**(−1), as described in Scheme 2.

Any dc oxidation processes that occur at more positive potential than about 0.5 V would be masked by the catalytic oxidation of ethanol that occurs with an onset potential of 0.54 V. In FTAC voltammetry, an additional well-defined oxidation process, not seen under dc conditions, is detected at 0.771 V. In FTAC voltammetry, the magnitudes of the peak currents associated with the ac harmonic components are highly sensitive to the kinetics of the heterogeneous electron transfer process[30] as well as the number of electrons transferred.[31] Since electron transfer processes involving $Ru^{IV}$ centers of **1** are fast (reversible or close to reversible),[19] the fact that the current magnitude associated with the process at 0.771 V is larger than for the **1**(−3)/**1**(−4) and **1**(0)/**1**(−1) processes and comparable to that found for the **1**(−1)/**1**(−3) process suggests that this process is likely to be a two-electron transfer process **1**(0)/**1**(2).

Dc voltammograms derived from 0.30 mM $[\mathbf{1}(\gamma\text{-}SiW_{10}O_{36})_2]^{10-}$ in methanol (Figure 9(a)) are similar to those obtained in ethanol. The **1**(0)/**1**(−1), **1**(−1)/**1**(−3) (this process is now slightly better resolved than in ethanol (Figure 8), and **1**(−3)/**1**(−4) processes have $E^{0\prime}$ values of 0.260, 0.097, and −0.173 V, respectively. Again, the **1**(0)/**1**(−1) process is more positive than the open-circuit potential, implying that the $Ru^{IV}$ center is spontaneously reduced by methanol. Under the FTAC voltammetric conditions, two well-defined oxidation processes with $E^{0\prime}$ values of 0.794 and 0.955 V are observed (Figure 9(b)). These two processes give rise to larger ac harmonic currents compared to other processes including the partially resolved **1**(−1)/**1**(−3) process. Therefore, these oxidation processes are again likely to be two-electron transfer processes leading to the formation of **1**(2) and **1**(4). The onset potential for methanol oxidation is 0.54 V. The oxidation current is much larger than for ethanol oxidation due to the involvement of **1**(4); e.g., under conditions of Figure 9(a) at 0.85 V, the methanol oxidation current is 17.9 versus 6.5 μA for ethanol (Figure 8(a)).

*3.2.2. Voltammetry of Surface-Confined* $[\mathbf{1}(\gamma\text{-}SiW_{10}O_{36})_2]^{10-}$. The voltammetry of surface-confined $[\mathbf{1}(\gamma\text{-}SiW_{10}O_{36})_2]^{10-}$ was also studied in alcohol solutions containing 0.50 M $H_2SO_4$ as the electrolyte using a $[\mathbf{1}(\gamma\text{-}SiW_{10}O_{36})_2]^{10-}$/PDDA-modified glassy carbon electrode. As shown in Figure 10, two surface-confined processes with $E^{0\prime}$ values of 0.278 and 0.096 V are observed in acidified methanol and ethanol media with similar characteristics to those observed for voltammograms of surface-confined $[\mathbf{1}(\gamma\text{-}SiW_{10}O_{36})_2]^{10-}$ in aqueous solution containing 1.0 M methanol or ethanol (Figure 5). No obvious processes were observed from the cyclic voltammogram obtained with a PDDA-modified glassy carbon electrode in ethanol solution. A similar voltammogram was obtained in methanol solution at a PDDA-modified glassy carbon electrode (not shown). The catalysis onset potentials are 0.6 V (vs $Fc/Fc^+$) for

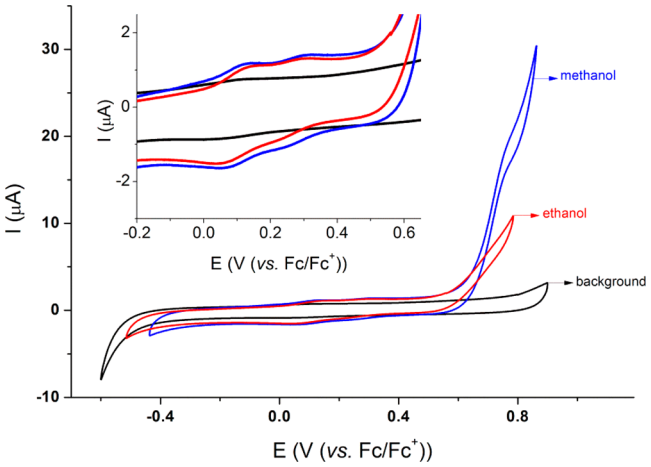


**Figure 10.** Cyclic voltammograms obtained at a 3.0 mm diameter glassy carbon electrode modified with 3 μL of $[\mathbf{1}(\gamma\text{-}SiW_{10}O_{36})_2]^{10-}$/PDDA (Γ = 0.03 nmol/cm$^2$) with a scan rate of 0.05 V s$^{-1}$ in ethanol (red line) and methanol (blue line) solutions containing 0.50 M $H_2SO_4$ as the electrolyte. Cyclic voltammogram obtained with a PDDA-modified glassy carbon electrode in ethanol solution is also shown for comparison (black line).

ethanol and methanol under conditions in Figure 10. However, the catalytic current for methanol is about 2.2-fold greater than for ethanol at 0.80 V even though the surface concentration of $[\mathbf{1}(\gamma\text{-}SiW_{10}O_{36})_2]^{10-}$ is comparable presumably due to the involvement of **1**(4) in the former case. By contrast, similar oxidation current magnitudes were found in aqueous 2.0 M $H_2SO_4$ solutions containing 1.0 M methanol or 1.0 M ethanol where **1**(1) is the catalytically active form (Figure 5).

**3.3. Bulk Electrolysis and Product Analysis.** The products of $[\mathbf{1}(\gamma\text{-}SiW_{10}O_{36})_2]^{10-}$-catalyzed ethanol and methanol oxidation were quantified after bulk electrolysis at carbon cloth electrodes in alcohol solutions containing 0.50 M $H_2SO_4$ as the electrolyte. In these experiments, the potential was held at 0.80 V (ethanol) and 0.93 V (methanol) under surface-confined conditions and hence slightly more positive than for the oxidation process **1**(0)/**1**(2). The current during bulk electrolysis remains constant for more than 15 h (Figure S4), which suggests that the catalyst is highly stable under the catalytic turnover conditions. The sharp decay in current observed at the beginning of the experiments is due to the double-layer charging process. The current obtained for oxidation of methanol is larger than that for ethanol, as expected on the basis of cyclic voltammetric data displayed in Figure 10. Bulk electrolysis experiments also were carried out at 0.66 V for ethanol and 0.83 V for methanol in alcohol solutions containing 0.10 mM $[\mathbf{1}(\gamma\text{-}SiW_{10}O_{36})_2]^{10-}$ and 0.50 M $H_2SO_4$ at the carbon cloth electrodes. Electrolysis products were collected after 100 C of charge had been passed and were analyzed by $^1H$ and $^{13}C$ NMR spectroscopy.

$^1H$ spectra obtained after bulk electrolysis in methanol using a $[\mathbf{1}(\gamma\text{-}SiW_{10}O_{36})_2]^{10-}$/PDDA-modified carbon cloth electrode with an applied potential of 0.93 V (vs $Fc/Fc^+$) (Figures S5(a) and (b)) show resonances with chemical shifts of 3.47, 3.54, 4.36, and 7.93 ppm. The singlet at 4.36 ppm indicates the formation of dimethoxymethane, while those at 3.54 (doublet) and 7.93 ppm (quartet) with a coupling constant of 0.74 Hz are assigned to methyl formate, confirmed by the detection of signals with the same characteristics after addition of 20 mM formic acid into methanol solution containing 0.50 M $H_2SO_4$, which formed


DOI: 10.1021/jacs.5b11408
J. Am. Chem. Soc. 2016, 138, 2617−2628

methyl formate with excess methanol as explained later. The singlet at 3.47 ppm which increased after bulk electrolysis is assigned to methyl hydrogen sulfate generated by reaction of methanol with sulfuric acid. Resonances at 5.03 ppm after bulk electrolysis and 5.11 ppm before bulk electrolysis are from $H_2O$. The increased intensity after bulk electrolysis is due to the formation of additional $H_2O$ during bulk electrolysis. The $^{13}C$ resonance (Figure S5(c)) with a chemical shift of 163.5 ppm also verifies the generation of methyl formate. Other expected resonances from dimethoxymethane and methyl formate have similar chemical shifts to those of the solvent methanol and hence are not detectable. Methanol oxidation to formaldehyde and formic acid followed by their reactions with excess methanol to form dimethoxymethane and methyl formate has been proposed by Serra et al.[32] to occur via the following series of reactions

$$CH_3OH \rightarrow H_2CO + 2H^+ + 2e^- \quad (3)$$

$$H_2CO + 2CH_3OH \rightarrow CH_2(OCH_3)_2 + H_2O \quad (4)$$

$$CH_3OH + H_2O \rightarrow HCOOH + 4H^+ + 4e^- \quad (5)$$

$$HCOOH + CH_3OH \rightarrow HCOOCH_3 + H_2O \quad (6)$$

NMR spectra also showed the formation of 1,1-diethoxyethane and ethyl acetate by reactions of excess ethanol with acetic acid and acetaldehyde, the 2- and 4-electron oxidation products of ethanol, respectively. $^1H$ spectra (Figures S6(a) and (b)) obtained after bulk electrolysis of ethanol using a $[\mathbf{1}(\gamma\text{-}SiW_{10}O_{36})_2]^{10-}$/PDDA-modified carbon cloth electrode with an applied potential of 0.80 V (vs $Fc/Fc^+$) contain a quartet with a chemical shift of 3.86 ppm and a coupling constant of 6.95 Hz and a singlet at 1.78 ppm that are characteristic of ethyl acetate. This assignment was confirmed by addition of 20 mM ethyl acetate to the solution after bulk electrolysis and the observation of an increase in intensity of both resonances. $^{13}C$ spectra (Figure S6(c)) also contained the carbonyl resonances expected for ethyl acetate at 172 ppm, confirmed by the detection of a signal with the same chemical shift after addition of 50 mM ethyl acetate into ethanol solution containing 0.50 M $H_2SO_4$. The quartet at 4.44 ppm with a coupling constant of 5.24 Hz is from the methanetriyl group of 1,1-diethoxyethane (acetaldehyde diethyl acetal). Other resonances expected for ethyl acetate and 1,1-diethoxyethane have chemical shifts close to those of the solvent ethanol and hence are not clearly defined. The reactions associated with ethanol oxidation to acetaldehyde and acetic acid followed by reactions with excess ethanol are proposed to be as follows

$$CH_3CH_2OH \rightarrow CH_3CHO + 2H^+ + 2e^- \quad (7)$$

$$CH_3CHO + 2CH_3CH_2OH \rightarrow CH_3CH(OCH_2CH_3)_2 + H_2O \quad (8)$$

$$CH_3CH_2OH + H_2O \rightarrow CH_3COOH + 4H^+ + 4e^- \quad (9)$$

$$CH_3COOH + CH_3CH_2OH \rightarrow CH_3COOCH_2CH_3 + H_2O \quad (10)$$

GC and GC-MS analysis also were undertaken to confirm the identities of the products. After bulk electrolysis using a $[\mathbf{1}(\gamma\text{-}SiW_{10}O_{36})_2]^{10-}$/PDDA-modified carbon cloth electrode, the solutions were distilled to separate the sulfuric acid supporting electrolyte and alcohol components. GC (Figure S7) and GC-MS results on the alcohol solutions confirm that the products of condensation with excess alcohol are methyl formate and dimethoxymethane and ethyl acetate and 1,1-diethoxyethane for methanol and ethanol oxidation, respectively. Diethyl ether and dimethyl ether were also detected but as products formed during the distillation of ethanol and methanol in the presence of sulfuric acid at an elevated temperature.[33]

Bulk electrolysis experiments were also carried out in acidic (2.0 M $H_2SO_4$) and neutral (0.40 M PB with 1.0 M $KNO_3$) aqueous media in the presence of 1.0 M methanol or ethanol. To increase the buffer capacity as required for exhaustive bulk electrolysis, 0.40 M PB solution was used in these experiments instead of 0.10 M as in the cyclic voltammetric studies. The potentials applied in these bulk electrolysis experiments were 0.7 V (ethanol) and 0.8 V (methanol) in 2.0 M $H_2SO_4$ solution and 0.4 V for both methanol and ethanol in 0.4 M PB solution (pH 7.0) with 1.0 M $KNO_3$.

Quantitative NMR experiments employed cyclohexane or *p*-toluenesulfonic acid as the internal standard in alcohol (Figure S8) or aqueous solutions (Figure S9) to quantify the concentrations of products formed. In alcohol solution, the $^1H$ NMR spectrum of cyclohexane gives a singlet at 1.26 ppm (with the $^1H$ of dimethyl sulfoxide-$d_6$ known to have a chemical shift of 2.5 ppm vs TMS), and *p*-toluenesulfonic acid in aqueous solution gives a singlet at 2.43 ppm together with two doublets around 7.41 and 7.73 ppm with a coupling constant of 8.05 Hz. Methyl formate, formic acid, ethyl acetate, and acetic acid exhibit similar resonances in aqueous and alcohol solutions. However, the NMR resonances of aldehydes are much more complicated in aqueous solution. Formaldehyde forms poly(oxymethylene) glycol and poly(oxymethylene) hemiformal in aqueous and methanolic solutions.[34,35] According to the literature,[34] the three $^1H$ resonances detected at 4.68, 4.78, and 4.88 ppm belong to the $CH_2O$ groups in the poly(oxymethylene) hemiformal formed in the presence of methanol. An increase in their intensity was found after addition of formaldehyde. In 0.40 M PB solution (pH 7.0) containing 1.0 M $KNO_3$, acetaldehyde gives a doublet at 2.27 ppm and a quartet at 9.71 ppm (coupling constant of 2.94 Hz), but in 2.0 M $H_2SO_4$ solution, acetaldehyde showed a broad resonance around 2 ppm due to the acid-catalyzed hydration according to the literature.[36−38]

In summary, only products of two- and four-electron reduction processes were observed under the conditions used in this study. That is, complete oxidation of alcohol to form $CO_2$ did not occur. Even though formate/formic acid also exhibits considerable reactivity upon electrooxidation at noble metal electrodes and has been proposed as a useful fuel in fuel cell applications,[39] further oxidation of formate/formic acid by **1** also was not observed under our conditions. To confirm the oxidized forms of $\mathbf{1}(0)$ are indeed inactive toward the oxidation of formate/formic acid under our experimental conditions, voltammetric studies were undertaken in both acidic and neutral aqueous electrolyte media containing 0.50 mM $[\mathbf{1}(\gamma\text{-}SiW_{10}O_{36})_2]^{10-}$ and 0.1 M sodium formate (Figure S10). Even though the concentration of formate/formic acid is now orders of magnitude higher, no catalytic current was observed, confirming the poor reactivity of formate/formic acid under these conditions.

**3.4. Catalytic Activity and Faradaic Efficiency (FE).** For quantitative determinations of product concentrations by NMR as needed to determine the catalytic activity and FE, baseline correction was undertaken prior to undertaking integrations. However, since it is difficult to use a broad NMR signal at 2 ppm for quantitative analysis of the acetaldehyde generated in 2.0 M



DOI: 10.1021/jacs.5b11408
J. Am. Chem. Soc. 2016, 138, 2617−2628

**Table 1. Comparison of Product Distribution and Catalytic Activities for Methanol and Ethanol Oxidation under Surface-Confined or Solution-Phase Bulk Electrolysis Conditions in Alcohol and Aqueous Media**

| | | | operational condition | | | product:catalyst ratio | | | |
|---|---|---|---|---|---|---|---|---|---|
| substrate | catalyst[a] | solvent/electrolyte | $E_{app.}$/V[b] | charge/C | reaction time/h | aldehyde | acid | FE (%) | ref |
| ethanol | **1*** | ethanol/0.50 M $H_2SO_4$ | 0.80 | 100 | 20.8 | 593[d] | 946[d] | 99.4 | this work |
| ethanol | **1**** | ethanol/0.50 M $H_2SO_4$ | 0.66 | 100 | 2.79 | 291.8 | 103.7 | 99.8 | this work |
| | CpRu(CO)($\mu$-I)($\mu$-dppm)$PtI_2$** | ethanol/0.10 M $[Bu_4N][BF_4]$ | 1.02 | 200 | 24 | 6 | [c] | 22.9 | [32] |
| | CpRu(CO)($\mu$-I)($\mu$-dppm)$PdI_2$** | ethanol/0.10 M $[Bu_4N][BF_4]$ | 1.02 | 200 | 24 | 8 | [c] | 30.2 | [32] |
| | CpRu(CO)($\mu$-I)($\mu$-dppm)$PtI_2$** | ethanol/0.10 M $[Bu_4N][BF_4]$ | 1.02 | 100 | [c] | 4.44 | [c] | 33.9 | [32] |
| | CpRu(CO)($\mu$-I)($\mu$-dppm)$PdI_2$** | ethanol/0.1 M $[Bu_4N][BF_4]$ | 1.02 | 100 | [c] | 4.95 | [c] | 37.3 | [32] |
| | **1**** | $H_2O$/2.0 M $H_2SO_4$ | 0.70 | 100 | 2.49 | 368 | 60 | 97.6 | this work |
| | **1**** | $H_2O$/0.40 M PB, pH 7.0, 1.0 M $KNO_3$ | 0.40 | 100 | 1.92 | 355 | 89 | 95.9 | this work |
| methanol | **1*** | methanol/0.50 M $H_2SO_4$ | 0.93 | 100 | 18.5 | 310[d] | 1071.5[d] | 98.1 | this work |
| methanol | **1**** | methanol/0.50 M $H_2SO_4$ | 0.83 | 100 | 2.0 | 149.6 | 164.8 | 95.8 | this work |
| | CpRu(CO)($\mu$-I)($\mu$-dppm)$PtI_2$** | methanol/0.10 M $[Bu_4N][BF_4]$ | 0.88 | 200 | 24 | 8.57 | 3.43 | 63.1 | [32] |
| | CpRu(CO)($\mu$-I)($\mu$-dppm)$PdI_2$** | methanol/0.10 M $[Bu_4N][BF_4]$ | 0.88 | 200 | 24 | 2.10 | 1.90 | 22.8 | [32] |
| | **1**** | $H_2O$/2.0 M $H_2SO_4$ | 0.80 | 100 | 1.56 | 170 | 157.4 | 96.9 | this work |
| | **1**** | $H_2O$/0.40 M PB, pH 7.0, 1.0 M $KNO_3$ | 0.40 | 100 | 7.12 | 178 | 151.8 | 96.3 | this work |

[a]Catalysts were either immobilized on the electrode surface (*) or dissolved in solution (**). [b]Reference electrodes were either $Hg/HgSO_4$ (for aqueous media) or $Fc/Fc^+$ (for alcohol media). [c]Not reported. [d]Calculated based on the total amount of the immobilized catalyst.

$H_2SO_4$ aqueous solution, HPLC was used to determine the concentration of this product after derivatization with 2,4-DNPH. In alcohol solutions containing 0.50 M $H_2SO_4$ as the supporting electrolyte, after bulk electrolysis (100 C of charge passed at a carbon cloth working electrode) under surface-confined catalytic conditions at a potential of 0.80 V (ethanol) or 0.93 V (methanol) (vs $Fc/Fc^+$), the products were found to be 38.5% and 22.4% of aldehydes and 61.5% and 77.6% of acids, respectively. When the bulk electrolysis was performed with 0.10 mM $[\mathbf{1}(\gamma\text{-}SiW_{10}O_{36})_2]^{10-}$ dissolved in ethanol or methanol containing 0.50 M $H_2SO_4$ as the supporting electrolyte, at an applied potential ($E_{app.}$) of 0.66 V (ethanol) or 0.83 V (methanol) (vs $Fc/Fc^+$), the product ratio of aldehyde increased to 73.8% and 47.6% for ethanol and methanol oxidation, respectively. The quantities of products formed were also measured for ethanol and methanol oxidation in the presence of 0.10 mM $[\mathbf{1}(\gamma\text{-}SiW_{10}O_{36})_2]^{10-}$ along with either 2.0 M $H_2SO_4$ or the combination of 1.0 M $KNO_3$ and 0.40 M PB solution (pH 7.0) as the supporting electrolytes. The total FE is 99% for ethanol and 98% for methanol oxidation under surface-confined conditions in alcohol solutions, while those in other cases are slightly lower but always above 94%. The data for product formation are summarized in Table 1 and compared with literature reports. It should be noted the total amount of $[\mathbf{1}(\gamma\text{-}SiW_{10}O_{36})_2]^{10-}$ rather than electrochemically active amount was used to calculate the product:catalyst ratios for the immobilized $[\mathbf{1}(\gamma\text{-}SiW_{10}O_{36})_2]^{10-}$. Therefore, the reported values are lower than their true values. Ideally, to compare the activity of different catalysts, commonly used performance indicators, such as turnover number (TON) and TOF should be used. Unfortunately, in the studies highlighted in Table 1, the products are mixtures, and the mechanism of acid formation in our study is unknown (see below), which means that unambiguously assigning quantitative values to TON/TOF is not possible. Nevertheless, it is clear that the polyoxometalate catalyst employed in our case is highly stable and active.

Bulk electrolysis experiments at glassy carbon working electrodes in methanol and ethanol with 0.10 M tetrabutylammonium tetrafluoroborate ($[Bu_4N][BF_4]$) as the supporting electrolytes were undertaken by Serra et al. with carbonyl-containing Ru and Fe heterobimetallic complex catalysts.[32] The Ru−Pt and Ru−Pd complexes, CpRu(CO)($\mu$-I)($\mu$-dppm)$PtI_2$ and CpRu(CO)($\mu$-I)($\mu$-dppm)$PdI_2$, were found to be the best, both catalyzing the oxidation of methanol in two- and four-electron oxidation manners to produce formaldehyde and formic acid, respectively. These products were found to react with methanol to give dimethoxymethane and methyl formate as the final products, respectively, as occurred in this work. However, the catalytic oxidation of ethanol only formed the two-electron oxidation product acetaldehyde which condensed with excess ethanol present to generate 1,1-diethoxyethane. By contrast, a significant amount of acid products were observed under all conditions when $[\mathbf{1}(\gamma\text{-}SiW_{10}O_{36})_2]^{10-}$ was used as the catalyst. Ethanol was postulated to be oxidized to acetic acid, assisted by $OH_{(ad)}$ species dissociated from $H_2O_{(ad)}$ on the surface of Pt(111).[3] The fact that $[\mathbf{1}(\gamma\text{-}SiW_{10}O_{36})_2]^{10-}$ also is a good catalyst for water oxidation suggests that this catalyst may provide an additional advantage in assisting alcohol oxidation into acid by facilitating the generation of $OH_{(ad)}$ species.

The FE obtained in the studies of Ru−Pt and Ru−Pd complexes[32] were significantly lower than that of $[\mathbf{1}(\gamma\text{-}SiW_{10}O_{36})_2]^{10-}$, being far below 50% under most conditions for alcohol oxidation. Furthermore, comparison of the $E_{app.}$ values, reaction duration, and the numbers of product per catalyst obtained from long-term electrolysis also reveal that $[\mathbf{1}(\gamma\text{-}SiW_{10}O_{36})_2]^{10-}$ is a far more active catalyst for alcohol oxidation than Ru−Pt and Ru−Pd complexes on both thermodynamic and kinetic bases. Waymouth and co-workers


DOI: 10.1021/jacs.5b11408
J. Am. Chem. Soc. 2016, 138, 2617−2628

reported the electrocatalytic oxidation of methanol to formate using an edge-plane graphite electrode modified with [($\eta^6$-*p*-cymene)($\eta^2$-*N*,*O*-(1*R*,2*S*)-*cis*-1-amino-2-indanol)]$Ru^{II}Cl$ in an aqueous medium containing 0.1 M $NaClO_4$ (pH = 11.5).[28] It was found that the catalytic process involves four electrons with a TOF of ~1 $s^{-1}$ based on the rotating disk electrode measurements (time scale of seconds instead of hours). Direct comparison of our catalyst with theirs is not straightforward since the reaction conditions (i.e., medium and duration) and techniques used are different. Although voltammetric experiments have also been undertaken under similar conditions (aqueous media containing 0.010 M NaOH and 1.0 M $NaNO_3$ or $KNO_3$, Figure 7), in our study long-term bulk electrolysis experiments were not undertaken since it was not possible to maintain constant pH. On the basis of the cyclic voltammetric data (Figure 7(d)), a TOF of ~0.2 $s^{-1}$ would be derived from the kinetic limiting current at −0.1 V if eq 11 is valid[40] and assuming the reaction is a two-electron transfer process ($n$ = 2).

$$I = nFA\Gamma^*\mathrm{TOF} \tag{11}$$

In eq 11, $F$ is Faraday's constant, and $A$ is the electrode area. It should be noted that eq 11 only estimates TOF. Although this TOF value is nominally smaller than that reported by Waymouth and co-workers,[28] it was achieved with 0.3 V lower overpotential. Importantly, $[\mathbf{1}(\gamma\text{-}SiW_{10}O_{36})_2]^{10-}$ exhibits remarkable activity over a wide pH range covering acidic, neutral, and alkaline conditions, which is also advantageous.

Methanol and ethanol oxidation to acid and aldehyde has been proposed to occur either via parallel pathways or through aldehydes as the intermediates.[3,41] The present results show that $[\mathbf{1}(\gamma\text{-}SiW_{10}O_{36})_2]^{10-}$ exhibits catalytic activity toward acetaldehyde and formaldehyde, while bare glassy carbon electrodes show no catalytic activity for acetaldehyde or formaldehyde as shown in Figure S11. Eqs 12 and 13 represent reactions for the oxidation of formaldehyde and its acetal to formic acid.

$$H_2CO + H_2O \rightarrow HCOOH + 2H^+ + 2e^- \tag{12}$$

$$CH_2(OCH_3)_2 + 2H_2O \rightarrow HCOOH + 2CH_3OH + 2H^+ + 2e^- \tag{13}$$

This result lends some support to the hypothesis that acid generation may proceed through the aldehyde oxidation pathway. The results in Table 1 show that considerable amounts of acid are produced which are often comparable to or even higher than for the aldehydes. These data imply that parallel pathways involving the direct oxidation of alcohol to acid must also take place. Otherwise, much smaller proportions of acids would be expected since the catalytic activities for the oxidation of alcohols and the corresponding aldehydes are both small and comparable (Figure S11), whereas the concentrations of alcohols are always much higher than aldehydes under conditions used for bulk electrolysis.

## 4. CONCLUSION

The molecular water oxidation catalyst $[\mathbf{1}(\gamma\text{-}SiW_{10}O_{36})_2]^{10-}$ exhibits high catalytic activity in electrooxidation of methanol and ethanol at carbon electrodes when dissolved in the solution phase or confined to the electrode surface. In both aqueous (over a wide pH range covering acidic, neutral, and alkaline) and alcohol media, the oxidized forms of $\mathbf{1}(0)$ quickly oxidize methanol and ethanol under all conditions investigated. Under these conditions, $\mathbf{1}(0)$ also shows considerable reactivity for the alcohols, especially in aqueous buffer solution at pH 7.0 in the presence of 1.0 M $NaNO_3$. Product analysis after bulk electrolysis showed that methanol and ethanol were oxidized to the relevant aldehydes and acids through two- and four-electron transfer pathways, respectively. The faradaic efficiencies for aldehyde and acid formation are greater than 94% under both surface-confined and solution-phase conditions. Long-term electrolysis data show no significant decline of catalytic current after passing 100 C of charge (>1000 electrons per catalyst), which confirms the high stability of $[\mathbf{1}(\gamma\text{-}SiW_{10}O_{36})_2]^{10-}$.

## ■ ASSOCIATED CONTENT

### Supporting Information

The Supporting Information is available free of charge on the ACS Publications website at DOI: 10.1021/jacs.5b11408.

Time-dependent voltammetric response of $[\mathbf{1}(\gamma\text{-}SiW_{10}O_{36})_2]^{10-}$ in aqueous 2.0 M $H_2SO_4$ medium (Figure S1); Cyclic and RDE voltammograms of $[\mathbf{1}(\gamma\text{-}SiW_{10}O_{36})_2]^{10-}$ in 0.10 M PB solutions (pH 7.0) containing 1.0 M $NaNO_3$ (Figure S2) or $KNO_3$ (Figure S3) in the presence and absence of 1.0 M alcohol; $I$–$t$ curves showing the stability of the catalysts (Figure S4); $^1H$ and $^{13}C$ NMR spectra obtained before and after electrolysis (Figures S5, S6, S8, and S9); Gas chromatograms of the electrolysis products (Figure S7); Cyclic voltammograms of $[\mathbf{1}(\gamma\text{-}SiW_{10}O_{36})_2]^{10-}$ obtained in the presence and absence of 0.1 M formate in acidic and neutral aqueous electrolyte media (Figure S10) and cyclic voltammograms of $[\mathbf{1}(\gamma\text{-}SiW_{10}O_{36})_2]^{10-}$/PDDA-modified glassy carbon electrodes in the presence of aldehyde or alcohol and in their absence (Figure S11) (PDF)

## ■ AUTHOR INFORMATION


### Corresponding Authors

*E-mail: alan.bond@monash.edu (A.M.B.).
*E-mail: jie.zhang@monash.edu (J.Z.).


### Notes

The authors declare no competing financial interest.

## ■ REFERENCES


(1) Vigier, F.; Rousseau, S.; Coutanceau, C.; Leger, J.-M.; Lamy, C. *Top. Catal.* **2006**, *40*, 111–121.
(2) Lamy, C.; Lima, A.; LeRhun, V.; Delime, F.; Coutanceau, C.; Léger, J.-M. *J. Power Sources* **2002**, *105*, 283–296.
(3) Asiri, H. A.; Anderson, A. B. *J. Electrochem. Soc.* **2015**, *162*, F115–F122.
(4) Iwasita, T. *Electrochim. Acta* **2002**, *47*, 3663–3674.
(5) Léger, J. M. *J. Appl. Electrochem.* **2001**, *31*, 767–771.
(6) Liu, H.; Song, C.; Zhang, L.; Zhang, J.; Wang, H.; Wilkinson, D. P. *J. Power Sources* **2006**, *155*, 95–110.
(7) Lamy, C.; Rousseau, S.; Belgsir, E. M.; Coutanceau, C.; Léger, J. M. *Electrochim. Acta* **2004**, *49*, 3901–3908.
(8) Chen, D.-J.; Tong, Y. J. *Angew. Chem. Int. Ed.* **2015**, *54*, 9394–9398.
(9) Dau, H.; Limberg, C.; Reier, T.; Risch, M.; Roggan, S.; Strasser, P. *ChemCatChem* **2010**, *2*, 724–761.
(10) Vannucci, A. K.; Hull, J. F.; Chen, Z.; Binstead, R. A.; Concepcion, J. J.; Meyer, T. J. *J. Am. Chem. Soc.* **2012**, *134*, 3972–3975.
(11) Pope, M. T. *Heteropoly and isopoly oxometalates*; Springer Verlag, 1983; Vol. *8*.
(12) Sadakane, M.; Steckhan, E. *Chem. Rev.* **1998**, *98*, 219–237.
(13) Bond, A. M. *Broadening Electrochemical Horizons*; Oxford Press: New York, 2002.
(14) Geletii, Y. V.; Botar, B.; Kögerler, P.; Hillesheim, D. A.; Musaev, D. G.; Hill, C. L. *Angew. Chem.* **2008**, *120*, 3960–3963.




DOI: 10.1021/jacs.5b11408
*J. Am. Chem. Soc.* 2016, 138, 2617–2628

(15) Sartorel, A.; Carraro, M.; Scorrano, G.; Zorzi, R. D.; Geremia, S.; McDaniel, N. D.; Bernhard, S.; Bonchio, M. *J. Am. Chem. Soc.* **2008**, *130*, 5006−5007.
(16) Toma, F. M.; Sartorel, A.; Iurlo, M.; Carraro, M.; Parisse, P.; Maccato, C.; Rapino, S.; Gonzalez, B. R.; Amenitsch, H.; Da Ros, T.; Casalis, L.; Goldoni, A.; Marcaccio, M.; Scorrano, G.; Scoles, G.; Paolucci, F.; Prato, M.; Bonchio, M. *Nat. Chem.* **2010**, *2*, 826−831.
(17) Guo, S.-X.; Liu, Y.; Lee, C.-Y.; Bond, A. M.; Zhang, J.; Geletii, Y. V.; Hill, C. L. *Energy Environ. Sci.* **2013**, *6*, 2654−2663.
(18) Lee, C.-Y.; Guo, S.-X.; Murphy, A. F.; McCormac, T.; Zhang, J.; Bond, A. M.; Zhu, G.; Hill, C. L.; Geletii, Y. V. *Inorg. Chem.* **2012**, *51*, 11521−11532.
(19) Liu, Y.; Guo, S.-X.; Bond, A. M.; Zhang, J.; Geletii, Y. V.; Hill, C. L. *Inorg. Chem.* **2013**, *52*, 11986−11996.
(20) Bond, A. M.; Duffy, N. W.; Guo, S.-X.; Zhang, J.; Elton, D. *Anal. Chem.* **2005**, *77*, 186 A−195A.
(21) Guo, S.-X.; Bond, A. M.; Zhang, J. *Rev. Polarogr.* **2015**, *61*, 21−32.
(22) Bond, A. M.; Elton, D.; Guo, S.-X.; Kennedy, G. F.; Mashkina, E.; Simonov, A. N.; Zhang, J. *Electrochem. Commun.* **2015**, *57*, 78−83.
(23) Bard, A. J.; Faulkner, L. R. *Eletrochemical Methods: Fundamental and Applications*, 2nd ed.; Wiley: New York, 2001.
(24) Eberson, L. *Electron Transfer Reactions in Organic Chemistry*; Springer-Verlag, 1987.
(25) Oldham, K. B.; Myland, J. C. *Fundamentals of Electrochemical Science*; Academic Press, Inc.: San Diego, 1994.
(26) Bard, A. J.; Parsons, R.; Jordan, J. *Standard potentials in aqueous solution*; CRC press, 1985; Vol. *6*.
(27) Anderson, A. B.; Asiri, H. A. *Phys. Chem. Chem. Phys.* **2014**, *16*, 10587−10599.
(28) Brownell, K. R.; McCrory, C. C. L.; Chidsey, C. E. D.; Perry, R. H.; Zare, R. N.; Waymouth, R. M. *J. Am. Chem. Soc.* **2013**, *135*, 14299−14305.
(29) Fleming, B. D.; Zhang, J.; Bond, A. M.; Bell, S. G.; Wong, L.-L. *Anal. Chem.* **2005**, *77*, 3502−3510.
(30) Guo, S.-X.; Zhang, J.; Elton, D. M.; Bond, A. M. *Anal. Chem.* **2003**, *76*, 166−177.
(31) O'Mullane, A. P.; Zhang, J.; Brajter-Toth, A.; Bond, A. M. *Anal. Chem.* **2008**, *80*, 4614−4626.
(32) Serra, D.; Correia, M. C.; McElwee-White, L. *Organometallics* **2011**, *30*, 5568−5577.
(33) Engineers, N. B. C. *Industrial Alcohol Technology Handbook*; Asia Pacific Business Press Inc., 2010.
(34) Hahnenstein, I.; Hasse, H.; Kreiter, C. G.; Maurer, G. *Ind. Eng. Chem. Res.* **1994**, *33*, 1022−1029.
(35) Gaca, K. Z.; Parkinson, J. A.; Lue, L.; Sefcik, J. *Ind. Eng. Chem. Res.* **2014**, *53*, 9262−9271.
(36) Scheithauer, A.; Grützner, T.; Rijksen, C.; Zollinger, D.; von Harbou, E.; Thiel, W. R.; Hasse, H. *Ind. Eng. Chem. Res.* **2014**, *53*, 8395−8403.
(37) Ahrens, M.-L.; Strehlow, H. *Discuss. Faraday Soc.* **1965**, *39*, 112−120.
(38) Socrates, G. *J. Org. Chem.* **1969**, *34*, 2958−2961.
(39) Yu, X.; Pickup, P. G. *J. Power Sources* **2008**, *182*, 124−132.
(40) Nakagawa, T.; Beasley, C. A.; Murray, R. W. *J. Phys. Chem. C* **2009**, *113*, 12958−12961.
(41) Hamnett, A. *Catal. Today* **1997**, *38*, 445−457.


DOI: 10.1021/jacs.5b11408
*J. Am. Chem. Soc.* 2016, 138, 2617−2628